Control of Interaction Strength in Hydrogen-Bonded Polymer Blends via the Density of the Hydroxyl Group

Chunlin Zhou,[†,‡] E. K. Hobbie,[*,†] B. J. Bauer,[†] Lipiin Sung,[†] Ming Jiang,[‡] and C. C. Han[†]

Polymers Division, National Institute of Standards and Technology, Gaithersburg, Maryland 20899, and Institute of Macromolecular Science, Fudan University, Shanghai, China 200433

Received July 22, 1997; Revised Manuscript Received November 20, 1997

ABSTRACT: Deuterium-labeled polystyrene modified by random distributions of the comonomer *p*-(1,1,1,3,3,3-hexafluoro-2-hydroxyisopropyl)-α-methylstyrene [DPS(OH)] has been blended with poly(butyl methacrylate) (PBMA) and studied with small-angle neutron scattering (SANS). Miscibility is induced via hydrogen bonding between the DPS(OH) hydroxyl group and PBMA carbonyl groups. As the density of the hydroxyl group increases, the susceptibilities of the related blends decrease, while those of the pure DPS(OH) increase. The extrapolated spinodal temperature increases linearly with comonomer density, and the hydrogen-bond enthalpy deduced from the SANS data is in good agreement with previously reported values.

I. Introduction

Hydrogen bonding is an effective way of making miscible blends out of otherwise immiscible polymer components.[1−11] If polymers A and B are immiscible over any practical range of temperature, miscibility can often be enhanced if, for example, polymer A is modified by the introduction of a random distribution of a comonomer that can form hydrogen bonds with B chain segments. The resulting blend is then a lower critical solution temperature (LCST) system with a composition-dependent interaction parameter. As discussed by Painter and co-workers,[12] the number of bonds that can form along a given A chain plays an important role in determining the phase behavior. The details of the distribution, however, may be less important.[9] In this paper, we use small-angle neutron scattering (SANS) to study the effect of hydrogen-bond density on the binding interaction in polystyrene/poly(butyl methacrylate) blends.

II. Experiment

A. Materials. The systems we consider are blends of modified, deuterium-labeled polystyrene [DPS(OH)] and poly(butyl methacrylate) (PBMA). The characteristics of the pure components are shown in Table 1, and the characteristics of the blends are shown in Table 2. To induce miscibility, the comonomer *p*-(1,1,1,3,3,3-hexafluoro-2-hydroxyisopropyl)-α-methylstyrene (HFMS) is introduced at random sites along the DPS chain. The OH group on HFMS forms hydrogen bonds with the carbonyl group on any PBMA segment (Figure 1). Random copolymer of deuterated styrene and HFMS was prepared using 2,2′-azoisobutyronitrile (AIBN) and toluene as the initiator and solvent, respectively.[2] The purified products were characterized by fluorine content, gel permeation chromatography (GPC), and infrared analysis and are denoted by DPS(OH)-*x*, where *x*/100 is the comonomer mole fraction or probability that a given styrene segment is modified by the presence of HFMS. For the DPS(OH)-*x* components listed in Table 1, the average number of OH's per chain (and standard deviation) determined by elemental fluorine analysis[13] is 5(±2), 6(±2), 16(±4), and 28(±5) for $x = 1$, 1.2, 3.5, and 10.1, respectively. (Error bars in graphs and uncertainties in quoted numerical results represent the best estimate of 2 standard deviations in experimental uncertainty.) PBMA-LL2 was prepared using AIBN and toluene as the initiator and solvent, respectively, fractionated in toluene and methanol, and characterized with GPC. The glass transition temperatures were determined using differential scanning calorimetry (DSC).

Table 1. Characteristics of the DPS(OH) and PBMA Components, Where M_w Denotes a Weight Average and M_n Denotes a Number Average over the Molecular Weight Distribution[a]

sample	M_w	M_n	M_w/M_n	T_g/°C
PBMA-LL2	71 000 ± 7100	51 000 ± 5100	1.39 ± 0.20	42 ± 3
DPS(OH)-1.0	61 500 ± 6100	34 300 ± 3400	1.83 ± 0.26	110 ± 3
DPS(OH)-1.2	60 300 ± 6000	33 400 ± 3300	1.81 ± 0.26	118 ± 3
DPS(OH)-3.5	53 700 ± 5400	28 200 ± 2800	1.91 ± 0.27	119 ± 3
DPS(OH)-10.1	36 000 ± 3600	21 000 ± 2100	1.71 ± 0.24	124 ± 3

[a] According to ISO 31−8, the term "Molecular Weight" has been replaced with "Relative Molar Mass" denoted by the symbol M_r. The conventional notation, rather than the ISO notation, has been used in this publication.

Table 2. Characteristics of the DPS(OH)/PBMA Blends, Where the Spinodal Temperature T_s Is Determined from the Double-Extrapolation Technique Described in the Text

blends	comp/wt %	T_g/°C	T_s/°C
DPS(OH)-1.0/PBMA-LL2	40/60	62 ± 5	136 ± 18
DPS(OH)-1.2/PBMA-LL2	40/60	63 ± 5	145 ± 18
DPS(OH)-3.5/PBMA-LL2	40/60	69 ± 5	307 ± 27
DPS(OH)-10.1/PBMA-LL2	40/60	71 ± 5	561 ± 53

B. SANS Measurements. Blends for SANS measurements were solvent cast from toluene, dried in a vacuum oven at 90 ± 1 °C for 2 days and at 110 ± 1 °C for 1 day, melt-pressed into 1-mm-thick disks, and annealed at 90 ± 1 °C for 12 h. The 40/60 DPS(OH)/PBMA composition [$\phi_0 = 0.38$, where ϕ_0 is the DPS(OH) volume fraction] is close to the (theoretical) "critical" composition $\phi_c = N_B^{1/2}/(N_A^{1/2} + N_B^{1/2}) \approx 0.5$, where the cubic term in a Landau expansion of the free energy of mixing vanishes.[9] Samples were transparent to visible light over the temperature range investigated in this study. SANS measurements were done on the 8-m instrument at the Cold Neutron Research Facility of the National Institute of Standards and Technology.

[†] National Institute of Standards and Technology.
[‡] Fudan University.

S0024-9297(97)01098-X CCC: $15.00
Published on Web 02/28/1998

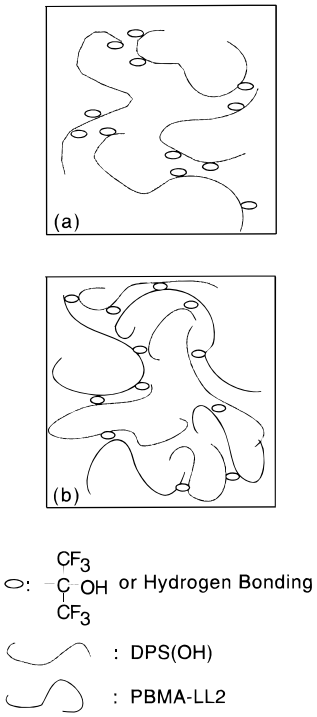

Figure 1. Schematic representation of the effect of hydrogen bonding in (a) pure DPS(OH) melts and in (b) DPS(OH)/PBMA blends.

III. Results and Discussion

A. Structure and Reversibility. Figure 2 shows the SANS structure factor, $S(q)$, for the four different DPS(OH)-x used in this study at $T = 140 \pm 0.5$ °C. Although the contrast is relatively weak in these pure melts, a systematic increase in the low-angle scattering intensity with hydrogen-bond density is evident. This is summarized in the inset, which shows the extrapolated zero-angle intensity (susceptibility) as a function of OH content. Since the OH groups are capable of forming hydrogen bonds with each other, this increase in scattering intensity probably reflects intra-interchain aggregation due to hydrogen bonding. Figure 3 shows $S(q)$ for 40/60 blends of the four DPS(OH)-x with PBMA-LL2 at $T = 120$ °C. In contrast to the pure melt behavior, the low-angle scattering shows a systematic increase with *decreasing* OH content. Due to dilution effects, the self-association of DPS(OH) segments can be ignored as a first approximation in the blends, and the decrease in scattering intensity with increasing hydrogen-bond density can be attributed to a suppression of composition fluctuations via physical cross-linking of the components.

It is interesting to note that the lower OH density scattering profiles ($x = 1.0$ and 1.2 in Figure 3) exhibit a broad peak in the "miscible-phase" structure factor. To investigate the reproducibility and stability of the low-q structure, we have performed consecutive heating and cooling runs as shown in Figures 4, 5, and 6 for $x = 1.2$, 3.5, and 10.1, respectively. All temperatures are below the apparent stability limit. After changing the temperature, the samples were annealed for 30 min before data collection began. In the lower OH density sample ($x = 1.2$, Figure 4), there is a significant increase in scattering intensity as the temperature is increased. After subsequent cooling to 110 °C, the system relaxes to the initial structure. The temperature dependence is considerably less in the higher OH content samples (Figures 5 and 6) and decreases with increasing hydrogen-bond density. The $x = 3.5$ (Figure 5) and $x = 10.1$ (Figure 6) samples show very slight hysteresis at very low q, but otherwise, the temperature dependence appears reversible.

B. Apparent Stability Limits. As in a previous study,[6] the miscible-phase scattering in these blends deviates from simple Lorentzian behavior below a cutoff

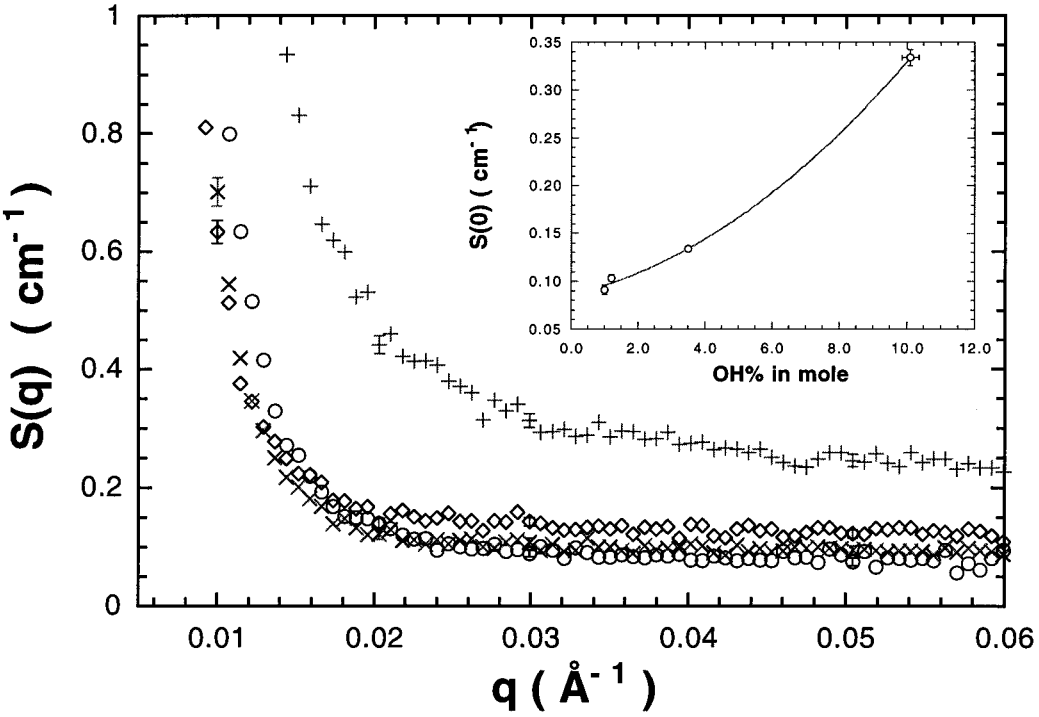

Figure 2. Structure factor $S(q)$ vs q for pure DPS(OH) melts at $T = 140$ °C for DPS(OH)-1.0 (○), DPS(OH)-1.2 (×), DPS(OH)-3.5 (◇), and DPS(OH)-10.1 (+). The inset shows how the extrapolated zero-angle intensity increases with the density of the OH group.

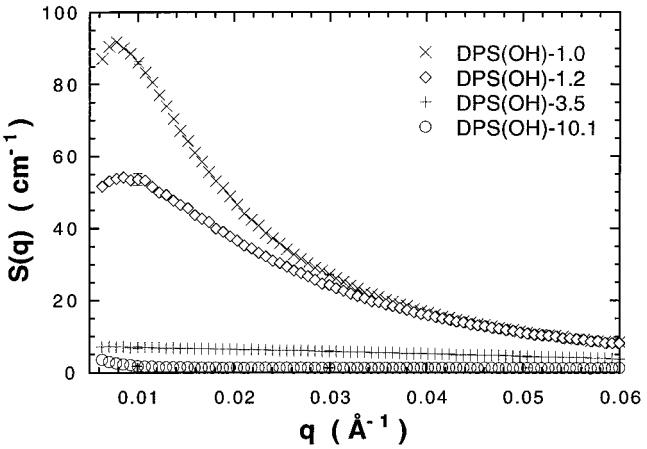

Figure 3. Structure factor $S(q)$ vs q for 40/60 DPS(OH)/PBMA blends at $T = 120$ °C. In contrast to the behavior exhibited by the pure DPS(OH) melts in Figure 2, the blends show an increase in low-angle scattering as the OH content decreases.

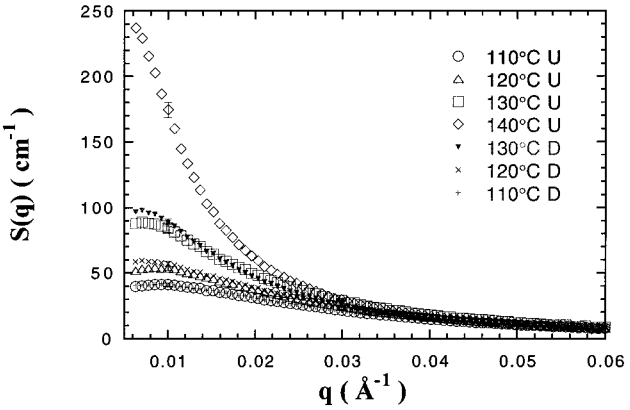

Figure 4. Demonstration of structural reversibility via heating and subsequent cooling of a 40/60 DPS(OH)-1.2/PBMA blend. The extrapolated spinodal temperature is 144.5 °C, and the sample was allowed to equilibrate for 30 min at each temperature. U denotes heating run and D denotes cooling run.

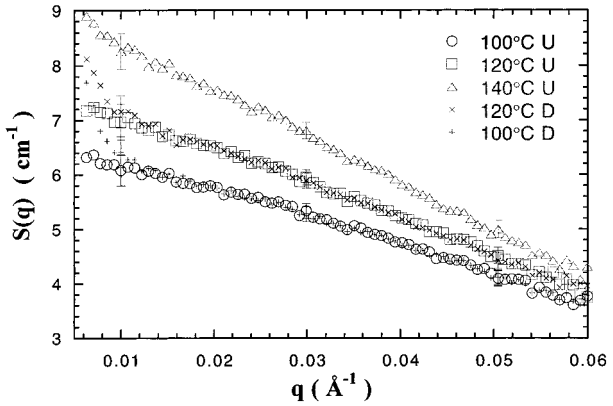

Figure 5. Heating/cooling run of a 40/60 DPS(OH)-3.5/PBMA blend. The extrapolated spinodal temperature corresponds to 307 °C, and the sample was equilibrated for 30 min at each temperature. The 100 °C data show slight evidence of hysteresis at very low q.

wavevector. The results of the previous section suggest that, for the molecular weights and hydrogen-bond densities under consideration here, this low-q structure may be associated with an equilibrium state. Information about the stability limit can be obtained from the temperature dependence of the susceptibility, S(0), and correlation length, ξ, that follow from a fit of the

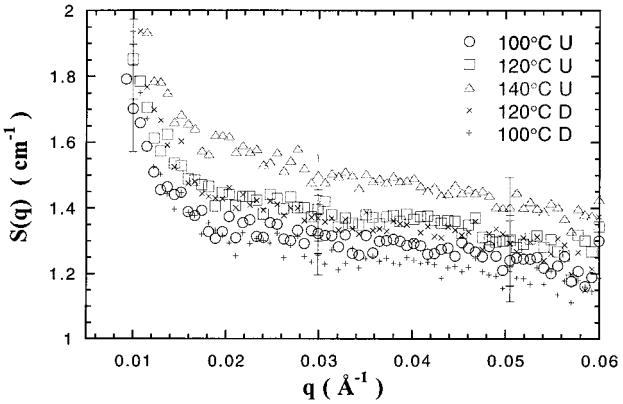

Figure 6. Heating/cooling run of a 40/60 DPS(OH)-10.1/PBMA blend. The extrapolated spinodal temperature corresponds to around 560 °C, and the sample was equilibrated for 30 min at each temperature. The 100 °C data again show slight evidence of hysteresis at very low q.

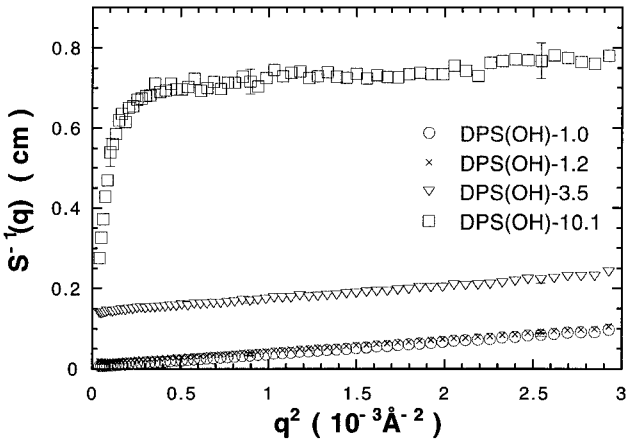

Figure 7. Zimm plots [$S^{-1}(q)$ vs q^2] of the 40/60 DPS(OH)/PBMA data shown in Figure 3. At low q, the blends show a systematic deviation from Ornstein−Zernike or Lorentzian behavior (eq 1) below a well-defined wavevector q_c. This deviation becomes more pronounced with increasing OH content.

intermediate-q data to the Ornstein−Zernike expression

$$S(q) = \frac{S(0)}{1 + \xi^2 q^2} \tag{1}$$

The fitting range for eq 1 was chosen to be 0.02 Å^{-1} < q < 0.045 Å^{-1}. A broad peak in the structure factor of the low-OH-density blends (Figure 3) appears at 0.01 Å^{-1}, corresponding to structures on the order of 10−100 nm. This suggests that the components are not randomly mixed over all length scales,[6,9] in contrast to what is generally observed in well-equilibrated homopolymer blends over the q range in question. Figure 7 shows Zimm plots of $1/S(q)$ vs q^2 for the four blends in Figure 3 at $T = 120$ °C.

In the present analysis, we ignore the low-q structure and focus on the intermediate-q range where eq 1 is applicable and the components appear randomly mixed. When there are, on average, n hydrogen-bond sites per DPS(OH) chain,[14] the inverse susceptibility becomes

$$\frac{k_N}{S(0)} = \frac{1}{N_A \nu_A \phi_0} + \frac{1}{N_B \nu_B (1 - \phi_0)} - 2\frac{\chi_{eff}(T)}{\nu_0} \tag{2}$$

where N is the degree of polymerization, v is the (molar)

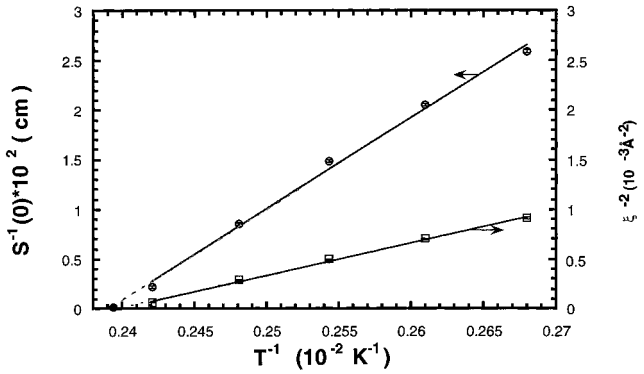

Figure 8. Double-extrapolation plot of the inverse susceptibility (left axis) and the inverse correlation length squared (right axis) vs $1/T$ for a 40/60 DPS(OH)-1.2/PBMA blend. The estimate of the apparent spinodal temperature is obtained by extrapolating these two quantities to zero.

segmental volume, k_N is the neutron scattering contrast factor, and ϕ_0 is the DPS(OH) volume fraction. The last term on the right-hand side of eq 2 represents the effective (Flory−Huggins) interaction parameter[9]

$$2\frac{\chi_{\text{eff}}(T)}{v_0} = 2\frac{\chi_0(T)}{v_0} - \frac{\phi_0}{N_A v_A}\ln K(n,T) \qquad (3)$$

where $\chi_0(T) = \chi_{0_1} + \chi_{0_2}/T$ is the "bare" homopolymer interaction parameter. If we represent hydrogen bonding by the chemical reaction A + B ⇄ AB, then the equilibrium constant $K(n,T) = [AB]/(v_0[A][B])$, where [X] denotes the number per unit volume of X, is proportional to $z_{AB}/z_A z_B$, where

$$z_j = \sum_m e^{-\epsilon_{jm}/k_B T}$$

is the "chain" partition function of the jth component (j = A, B, AB), ϵ_{jm} being the energy of the mth configuration of species j. We consider a simple model with $K(n,T) = W_n \exp(nh/k_B T)$ and $W_n = \Omega_{AB}(n)/\Omega_A\Omega_B$, where h is the enthalpy of a single hydrogen bond and Ω_X denotes the number of distinguishable states of type X within the volume v_o. Such a model ignores the self-association of A due to hydrogen bonding. We note that the equilibrium constant $K(n,T)$ has no physical meaning for $n = 0$, and we adopt the convention $\Omega_{AB}(0) = \Omega_A\Omega_B$ so that the effective hydrogen-bond interaction is zero for $n = 0$.

Based on eqs 2 and 3, the inverse susceptibility and inverse correlation length squared should be of the form $a + b/T$, with

$$-a = 2\frac{\chi_{0_1}}{v_0} - \left\{\frac{1}{N_A v_A \phi_0} + \frac{1}{N_A v_A(1-\phi_0)}\right\} - \frac{\phi_0}{N_A v_A}\ln W_n \qquad (4)$$

and

$$b = 2\frac{|\chi_{0_2}|}{v_0} + \frac{h\phi_0}{v_A k_B}\left(\frac{n}{N_A}\right) \qquad (5)$$

with the extrapolated spinodal temperature given as $T_s = -b/a$. An example of this type of double linear extrapolation plot is shown in Figure 8. From the slope, b, and intercept, a, of such plots as a function of hydrogen-bond density (Figure 9), we get information

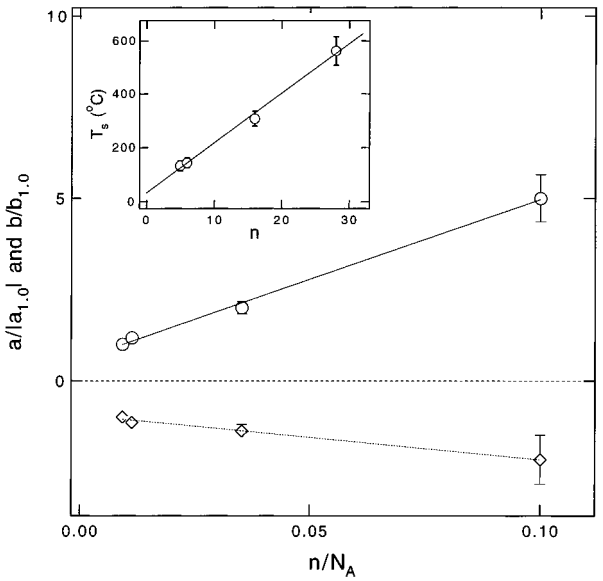

Figure 9. Slope (b, open circles−solid line) and intercept (a, open diamonds−dashed line) of $S^{-1}(0)$ vs $1/T$ as a function of n/N_A, where a and b have been reduced by the absolute values of their $x = 1.0$ values. The inset shows the extrapolated spinodal temperature as a function of the average number of hydrogen bonds per DPS(OH) chain (n). The lines are linear fits of the data.

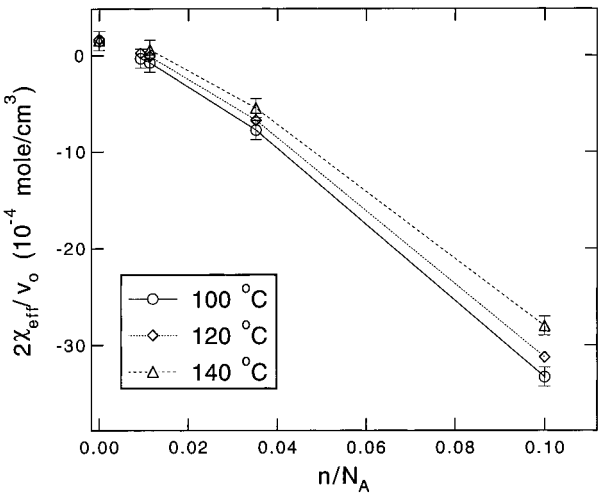

Figure 10. Effective Flory−Huggins interaction parameter $2\chi_{\text{eff}}/v_0$ as a function of OH content at three different temperatures. The data for $n = 0$ are from ref 15.

about the n dependence of the entropic and enthalpic terms as well as the dependence of the extrapolated spinodal temperature on hydrogen-bond density (inset Figure 9). In Figure 9, the b values have been reduced by $b_{1.0} = 0.433$ mol/cm^3 and the a values have been reduced by $|a_{1.0}| = 1.057 \times 10^{-3}$ mol/cm^3. From eq 2, we can calculate the effective Flory−Huggins interaction parameter $2\chi_{\text{eff}}/v_0$, which is shown as a function of OH content in Figure 10. For reference, $n = 0$ values from a previous SANS study of lower molecular weight DPS/PBMA blends[15] are also shown in Figure 10.

Neglecting changes in the homopolymer interaction parameter associated with the systematic decrease in N_A with increasing OH content,[16] the data shown in Figure 9 are quite informative. The enthalpic part, b, shows a linear increase with n/N_A as predicted by eq 5. The slope (vs n/N_A) of 19 mol/(cm^3 K) implies $h = 9 \pm 2$ kcal/mol, which is in order-of-magnitude agreement

with hydrogen-bond enthalpies of 6 kcal/mol reported elsewhere.[17] Although we have not made a quantitative prediction, the n dependence of the intercept (a or the "entropic" term) is fairly intuitive. The data suggest that $\ln(W_n^{-1}) = \ln(\Omega_A\Omega_B/\Omega_{AB})$ is a slowly *increasing* function of n. This implies that the loss of conformational states associated with site-specific binding of A and B chains more than offsets the increase in $\Omega_{AB}(n)$ associated with different bond configurations.

Even in the absence of self-association, our model is an approximate approach that neglects important factors such as the loss of local (predominantly rotational) degrees of freedom due to hydrogen bonding. The bond enthalpy in the above analysis should thus be viewed as an empirical parameter, and the inclusion of higher order effects would likely reduce the value of h deduced from the measurements and improve agreement with the accepted value.

IV. Conclusions

In conclusion, we have used SANS to study the dependence of the effective hydrogen-bond interaction parameter on the density of the hydrogen-bonding comonomer or, equivalently, the average number of hydroxyl groups per polystyrene chain. The results are in good agreement with a simple physical picture of the binding interaction.

Acknowledgment. We acknowledge useful discussions with E. Amis.

References and Notes

(1) Pearce, E. M.; Kwei, T. K.; Min, B. Y. *Macromol. Sci., Cem.* **1981**, *A21*, 1181.
(2) Cao, X.; Jiang, M.; Yu, T. *Makromol. Chem.* **1989**, *190*, 117.
(3) Jiang, M.; Cao, X.; Chen, W.; Xiao, H.; Jin, X.; Yu, T. *Makromol. Chem. Macromol. Symp.* **1990**, *38*, 161.
(4) Jiang, M.; Chen, W.; Yu, T. *Polymer* **1991**, *32*, 984.
(5) Qiu, X.; Jiang, M. *Polymer* **1994**, *35*, 5084.
(6) Hobbie, E. K.; Bauer, B. J.; Han, C. C. *Phys. Rev. Lett.* **1994**, *72*, 1830.
(7) Hobbie, E. K.; Merkle, G.; Bauer, B. J.; Han, C. C. *Phys. Rev. E* **1995**, *52*, 3256.
(8) Merkle, G.; Bauer, B. J.; Han, C. C. *J. Chem. Phys.* **1996**, *104*, 9647.
(9) Hobbie, E. K.; Han, C. C. *J. Chem. Phys.* **1996**, *105*, 738. Hobbie, E. K.; Han, C. C. *J. Chem. Phys.* **1997**, *107*, 2162.
(10) Hobbie, E. K.; Merkle, G.; Bauer, B.; Han, C. C. *Mod. Phys. Lett. B* **1996**, *25*, 1219.
(11) He, M.; Liu, Y.; Feng, Y.; Jiang, M.; Han, C. C. *Macromolecules* **1991**, *24*, 464.
(12) Painter, P. C.; Park, Y.; Coleman, M. M. *Macromolecules* **1989**, *22*, 570, 580. Coleman, M. M.; Lickhus, A. M.; Painter, P. C. *Macromolecules* **1989**, *22*, 586.
(13) This analysis was carried out by Galbraith Laboratories, Inc. Certain commercial equipment, instruments, materials, or laboratories are identified in this article in order to adequately specify the experimental procedure. Such identification does not imply recommendation or endorsement by the National Institute of Standards and Technology nor does it imply that materials, equipment, or services identified are necessarily the best available for the purpose.
(14) We ignore the effect of interchain polydispersity in the binding interaction, as this appears to be of secondary importance. The inhomogeneous nature of the binding interaction, however, may be important. See ref 9.
(15) Hammouda, B.; Bauer, B. J.; Russell, T. P. *Macromolecules* **1994**, *27*, 2357.
(16) As a next approximation, we might expect the homopolymer interaction parameter $\chi_0(T) = \chi_{01} - |\chi_{02}|/T$ to decrease with decreasing N_A. In this scenario, χ_{01} would decrease while $|\chi_{02}|$ would be relatively insensitive to changes in N_A.
(17) Kwei, T. K.; Pearce, E. M.; Ren, F.; Chen, J. P. *J. Polym. Sci., Phys. Ed.* **1986**, *24*, 1597.

MA971098D